Monatsh Chem (2011) 142:961–971
DOI 10.1007/s00706-011-0497-3

ORIGINAL PAPER

Systematic investigation on the binding of GW420867X as HIV-1 reverse transcriptase inhibitor

Patchreenart Saparpakorn · Peter Wolschann · Alfred Karpfen · Pornpan Pungpo · Supa Hannongbua

Received: 17 October 2010 / Accepted: 30 March 2011 / Published online: 4 May 2011

Abstract The interactions between ligands and the surrounding binding site depend on the different contributions of individual amino acids. The determination of these particular interaction energies is sensitive to the model used, i.e., which part of the amino acids is taken into account and which terminating procedure is applied. In this study, the subtle interaction between individual residues from the HIV-1 reverse transcriptase allosteric binding site and an inhibitor, isopropyl (*S*)-2-ethyl-7-fluoro-3,4-dihydro-3-oxoquinoxalin-1(2*H*)-carboxylate (GW420867X), was investigated by using high-level quantum chemical calculations (MP2, M06-2X, and B3LYP) with the following basis sets: 6-31G(d), 6-31G(d,p), 6-311G(d), and 6-311G(d,p). The results obtained indicate that the interaction between the inhibitor and Lys101 is the most important one for the binding. We have calculated this interaction using various models to evaluate the effect of neighboring residues. Electrostatic interactions induced by the terminating substituents were also studied using natural population analysis. The results show that even systems where the amide bond is cut and capped with hydrogen atoms can be used as reliable models for estimating the individual interaction energies. Furthermore, the interaction energies of GW420867X in wild-type and Lys101Glu mutant are also investigated to explain the loss of GW420867X's activity in the Lys101Glu mutant.

Keywords NNRTI · HIV-1 RT · MP2 · M06-2X · Interaction energy

P. Saparpakorn (✉) · S. Hannongbua
Department of Chemistry, Faculty of Science,
Kasetsart University, Bangkok 10900, Thailand
e-mail: fscipnsk@ku.ac.th

P. Saparpakorn · S. Hannongbua
Center of Nanotechnology KU, Kasetsart University,
Bangkok 10900, Thailand

P. Saparpakorn
International Center for Science and Engineering
Programs (ICSEP), Faculty of Science and Engineering,
Waseda University, Tokyo 169-8555, Japan

P. Wolschann · A. Karpfen
Institute of Theoretical Chemistry,
University of Vienna, Vienna, Austria

P. Pungpo
Department of Chemistry, Faculty of Science,
Ubonratchathani University, Ubonratchathani 34190, Thailand

Introduction

The reverse transcriptase (RT) of human immunodeficiency virus type-1 (HIV-1) is the essential enzyme converting the single-stranded viral RNA genome into double-stranded proviral DNA prior to its integration into the host genomic DNA [1]. HIV-1 RT is an asymmetric heterodimer consisting of a 560-residue chain (p66 subunit) and a 440-residue chain (p51 subunit). Each subunit consists of four subdomains called fingers, palm, thumb, and connection. Moreover, the C-terminal 120 amino acids in the p66 unit form the RNaseH domain. The polymerase site consisting of three subdomains, fingers, palm, and thumb, is located at the N-terminal in the p66 unit [2, 3]. HIV-1 RT inhibitors can be categorized into three types: nucleoside reverse transcriptase inhibitors (NRTIs), nucleotide reverse transcriptase inhibitors (NtRTIs), and nonnucleoside reverse transcriptase inhibitors (NNRTIs) [4]. NRTIs and NtRTIs bind at the catalytic site, while NNRTIs bind at a hydrophobic pocket that is about 10 Å away from the

enzyme's active site in the p66 subunit. NNRTIs, such as nevirapine, efavirenz, etravirine, TMC-278, and GW420867X, are interesting for developing novel potent inhibitors because of their high sensitivity and high specificity [5]. However, rapid development of drug resistance occurs, caused by mutation, e.g., Leu100Ile, Lys103Asn, and Tyr181Cys [6].

Nowadays, nevirapine, delavirdine, efavirenz, and etravirine have been approved as NNRTIs by the Food and Drug Administration [7]. Isopropyl (*S*)-2-ethyl-7-fluoro-3,4-dihydro-3-oxoquinoxalin-1(2*H*)-carboxylate (GW420867X) is a second-generation NNRTI showing significantly improved activity against Leu100Ile, Lys101Glu, and Tyr188Cys HIV-1 RT, as compared with first-generation inhibitors [8]. GW420867X reveals 1.4 ± 0.6, 2.5 ± 0.7, and 2.4-fold resistances with Leu100Ile, Lys101Glu, and Tyr188Cys HIV-1 RT as compared with wild-type HIV-1 RT. The complex structure of GW420867X/wild-type HIV-1 RT is shown in Fig. 1. The crystal structure reveals that GW420867X binds to the NNRTI binding pocket and forms a relatively strong hydrogen bond with Lys101. Therefore, GW420867X is an interesting inhibitor to study the modes of binding to both wild-type and mutant-type proteins.

To elucidate the binding of NNRTIs in the HIV-1 binding pocket, quantum chemical calculations are applied to determine the interaction energies between NNRTIs and the residues surrounding the binding pocket. These methods have been used successfully in the past to study binding phenomena. Nunrium et al. [9] calculated the particular interaction energies of efavirenz in the HIV-1 RT binding pocket based on the B3LYP/6-31G(d,p) method. In structures of HIV-1 RT/8-Cl (+)-(*S*)-4,5,6,7-tetrahydro-8-chloro-5-methyl-6-(3-methyl-2-butenyl)-imidazo[4,5,1-*jk*]-[1,4]benzodiazepine-2(1*H*)-thione (TIBO) the binding interaction was studied using B3LYP/6-31G(d,p) and MP2/6-31G(d,p) methods [10]. In their models, the N- and C-terminal of each residue were capped by using acetyl (CH_3CO–) and methylamino groups (–$NHCH_3$). The geometries of the caps were obtained from the backbone of the adjacent amino acid. Moreover, quantum chemical calculations based on the molecular fractionation with conjugate caps (MFCC) method was also applied to study the interaction energies of efavirenz [11] and nevirapine [12] in wild-type and mutant types of HIV-1 RT using a combination of HF/3-21G, B3LYP/6-31G(d), and MP2/6-31G(d) levels. A pair of conjugated groups (CH_3CO– and –$NHCH_3$) is used to cap the residues. However, their calculated interaction energies are considered to exclude the energies resulting from the caps. The results [9–12] revealed that interaction energies calculated using the B3LYP and MP2 methods can be used to explain the binding of NNRTI in the HIV-1 RT binding pocket. Due to the lack of dispersion forces in the B3LYP method, Truhlar et al. [13] developed a new density functional method called M06-2X. This method showed good performance when applied to noncovalent interactions, especially for π–π stacking [14–16]. Other calculations that can prove useful to elucidate the binding phenomenon are atomic charge calculations [17–20]. Several methods based on population analysis were applied to derive the atomic charges, e.g., natural population analysis (NPA), which can be used to rationalize electrostatic interactions [21].

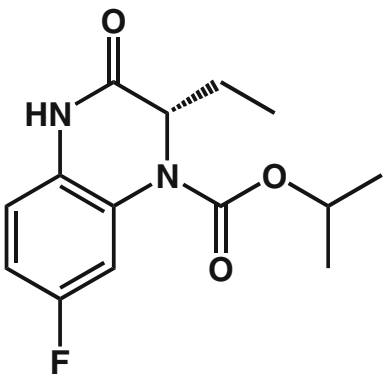

Fig. 1 Structure of GW420867X

The aim of the present work is to study the residue interaction energies between GW420867X and the surrounding amino acids of the binding pocket. In detail, the main attractive interaction with Lys101 is investigated using various models to terminate the free valences of the amino acids. The models are constructed to study the effects of adjacent residues, side-chain atoms, and terminal atoms attached to Lys101. Electrostatic interactions are considered by using various charge calculations. Finally, the interaction energies of GW420867X in wild-type and Lys101Glu mutant are also compared.

Results and discussion

Validation of the basis set

The individual interaction energies of GW420867X and the amino acids of the binding pocket calculated using B3LYP, M06-2X, and MP2 methods with 6-31G(d), 6-31G(d,p), 6-311G(d), and 6-311G(d,p) basis sets are presented in Table 1. All calculations demonstrate that the main contribution of the attractive interaction to GW420867X within the binding pocket is the interaction with Lys101. The interaction energies are around −65.3 to −66.5 kJ/mol, −77.8 to −80.8 kJ/mol, and −66.5 to −68.2 kJ/mol for the different basis sets in B3LYP, M06-2X, and MP2. From the orientation of GW420867X in the HIV-1 RT binding site (pdb code 2opp, as shown in Fig. 2), a hydrogen bond between an oxygen and the nitrogen atom of backbone Lys101 was found. All methods also reveal attractive interactions to Lys103 with −20.1 to −20.5 kJ/mol, −25.1

Table 1 Interaction energies between GW420867X and surrounding residues using B3LYP, M06-2X, and MP2 methods with different basis sets [the amino acids are cut at the –(C=O)–NH– connection]

Residue	Interaction energy (kJ/mol)											
	B3LYP				M06-2X				MP2			
	6-31G(d)	6-31G(d,p)	6-311G(d)	6-311G(d,p)	6-31G(d)	6-31G(d,p)	6-311G(d)	6-311G(d,p)	6-31G(d)	6-31G(d,p)	6-311G(d)	6-311G(d,p)
Pro95	10.9	10.9	10.9	10.9	4.2	3.8	3.3	3.8	8.4	6.7	7.1	5.0
Leu100	24.7	24.3	25.1	24.7	−10.0	−11.3	−14.2	−14.2	0.8	−2.9	−3.8	−8.4
Lys101	−65.3	−65.3	−66.5	−65.7	−78.2	−77.8	−80.8	−79.9	−68.2	−67.8	−66.9	−66.5
Lys103	−20.1	−20.1	−20.1	−20.5	−25.1	−25.5	−26.8	−26.8	−26.8	−27.2	−28.0	−28.9
Val106	8.4	8.4	8.4	8.4	−5.0	−5.4	−7.1	−7.1	−3.8	−5.0	−6.3	−7.9
Val179	5.0	5.0	5.4	5.0	−9.2	−10.0	−11.3	−11.3	−3.8	−5.4	−5.4	−7.5
Tyr181	4.6	4.6	4.6	4.2	−10.5	−10.9	−13.4	−13.0	−10.0	−10.9	−12.6	−13.8
Tyr188	7.5	7.5	7.9	7.5	−7.5	−7.9	−10.0	−10.0	−7.9	−9.2	−10.9	−12.6
Gly190	1.3	1.3	1.7	1.7	−3.8	−4.2	−4.2	−3.8	−1.3	−1.7	−1.7	−2.5
Phe227	0.8	0.8	0.4	0.4	−1.3	−1.3	−2.1	−2.1	−2.5	−2.5	−2.9	−2.9
Trp229	5.9	5.9	5.4	5.4	−10.5	−10.9	−13.8	−13.4	−7.1	−8.4	−10.9	−12.1
Leu234	4.6	4.6	5.4	5.0	−4.2	−4.6	−5.4	−5.4	−5.4	−6.3	−6.3	−7.5
His235	−4.2	−4.2	−4.6	−4.6	−7.5	−7.5	−7.9	−7.9	−6.7	−6.3	−6.7	−6.3
Tyr318	−1.7	−1.7	−2.5	−2.1	−7.9	−7.9	−10.0	−9.6	−10.0	−10.0	−11.7	−11.7

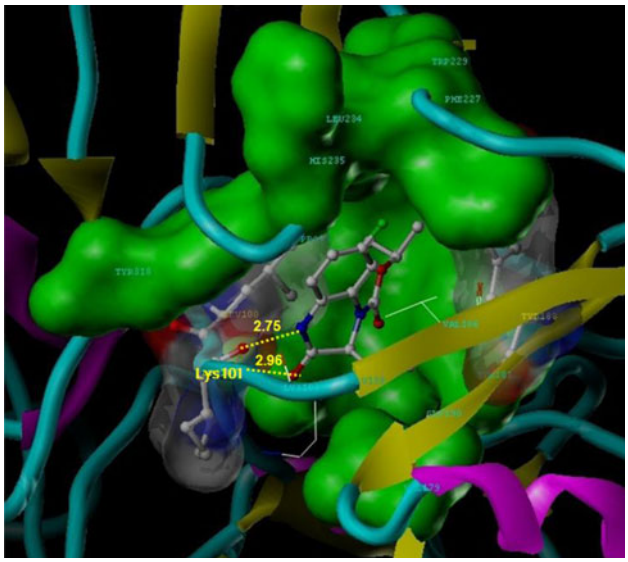

Fig. 2 Orientation of GW420867X in HIV-1 RT binding site

to −26.8 kJ/mol, and −26.8 to −28.9 kJ/mol for B3LYP, M06-2X, and MP2. The M06-2X and MP2 results show that GW420867X is also bound in the HIV-1 RT binding pocket with other, smaller attractive interactions to Val106, Val179, Tyr181, Tyr188, Trp229, Leu234, His235, and Tyr318. All M06-2X and MP2 interaction energies are lower than those obtained by B3LYP. Both methods yield similar interaction energies. However, the M06-2X interaction energies with Leu100 and Lys101 are about 5.8–10.9 kJ/mol and 10.0–13.8 kJ/mol larger than the MP2 values. Especially the interaction to Leu100, calculated with M06-2X and MP2, is lower by about 33–38 and 25–33 kJ/mol as compared with the B3LYP method. This finding is in agreement with the results from Tsuzuki and Lüthi [22]. They found that BLYP and B3LYP methods do not include the dispersion contribution properly. Furthermore, H–π or π–π interactions (i.e., Tyr181, Tyr188, Trp229, and Tyr318) are better described by M06-2X and MP2 than by B3LYP. Our results agree well with previous publications that M06-2X and MP2 is superior in the case of H–π or π–π interactions [15, 23, 24].

When the basis set was increased, the interaction energies compared with the 6-31G(d) basis did not change significantly (±0.8 kJ/mol for B3LYP, <4 kJ/mol for M06-2X). In the case of MP2, the differences of the interaction energies compared with the 6-31G(d) basis set are about ±5.0 kJ/mol, except for Leu100 [9.2 kJ/mol using 6-311G(d,p) basis set]. Because the differences in interaction energies are quite insensitive to basis set modifications, the 6-31G(d) basis set was used in the following to reduce computation times.

Effects of proximate residues

To study the attractive interaction of GW420867X to Lys101 in detail, models including the residues adjacent to Lys101 (i.e., Gly99, Leu100, Lys102, and Lys103) were calculated, as shown in Table 2. Models of each residue interacting with GW420867X are shown in Fig. 3. Selected distances (in Å) are also given in Fig. 3 to explain the attractive or repulsive interactions. Model1-Lys101 reveals strong H-bonding

Table 2 Interaction energies between GW420867X and Lys101 and nearby residues

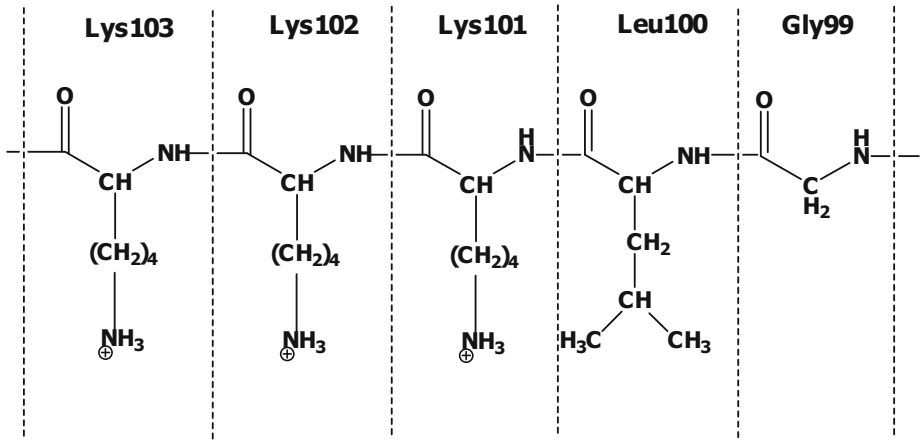

Model	Residue					Interaction energy (kJ/mol)		
						B3LYP/6-31G(d)	M06-2X/6-31G(d)	MP2/6-31G(d)
Model1-Lys101			Lys101			−65.3	−78.2	−68.2
Model1-Leu100				Leu100		24.7	−10.0	0.8
Model1-Lys102		Lys102				6.3	5.9	4.6
Model1-Gly99					Gly99	2.5	2.5	1.7
Model1-Lys103	Lys103					−20.1	−25.1	−26.8
Model2-1			Lys101	Leu100		−43.5 (−2.9)[a]	−89.5 (−1.3)	−70.7 (−3.3)
Model2-2		Lys102	Lys101			−65.3 (−6.3)	−78.7 (−6.3)	−69.9 (−6.3)
Model3-1		Lys102	Lys101	Leu100		−43.5 (−9.2)	−90.0 (−7.5)	−73.2 (−10.5)
Model3-2			Lys101	Leu100	Gly99	−41.4 (−3.3)	−87.0 (−1.3)	−69.0 (−3.3)
Model3-3	Lys103	Lys102	Lys101			−84.9 (−7.9)	−102.5 (−5.0)	−96.2 (−5.9)
Model4-1		Lys102	Lys101	Leu100	Gly99	−41.4 (−9.6)	−87.9 (−7.9)	−71.5 (−10.5)
Model4-2	Lys103	Lys102	Lys101	Leu100		−60.7 (−6.3)	−112.1 (−4.6)	−97.5 (−7.9)
Model5-1	Lys103	Lys102	Lys101	Leu100	Gly99	−57.7 (−5.9)	−108.8 (−3.8)	−95.0 (−7.1)

[a] Energy difference, as compared with the sum of each residue

between the hydrogen atom and an oxygen atom of the quinoxaline ring and an oxygen and a hydrogen atom of the backbone of Lys101. The distance between an oxygen atom at the quinoxaline ring and a hydrogen atom of the ammonium group of Lys101 was found to be 4 Å. In model1-Gly99 and model1-Lys102, there is no attractive interaction between GW420867X and these residues. In case of model1-Leu100, there may be a repulsive interaction between the dimethyl group of Leu100 and GW420867X. In addition, a further attractive interaction was also detected from the H-bonding between C_β of Leu100 and a nitrogen atom of quinoxaline ring and the H–π interaction between C_δ of Leu100 and a phenyl ring of quinoxaline ring. In model1-Lys103, weak hydrogen bonds between GW420867X and Lys103 were found, as shown in Fig. 3e.

As compared with the individual interaction energies of nearby residues, Gly99, Leu100, Lys102, and Lys103 showed no interaction, repulsive, slightly repulsive, and attractive interaction, with B3LYP/6-31G(d). In the case of M06-2X/6-31G(d), GW420867X has an attractive interaction with Leu100 and Lys103 and no interaction with Gly99 and Lys102. For MP2/6-31G(d), no bonding interaction was found for Gly99, Leu100, and Lys102. An attractive interaction to Lys103 was observed in GW420867X. When a nearby residue was added (models2-1 and 2-2), the interaction energies of these models were not significantly different from the sum of individual residues. The interaction energies were also compatible with the models with two, three, and four nearby residues. The interaction energies of these models were lower than those of the sum of each residue by about −2.9 to −9.6 kJ/mol, −1.3 to −7.9 kJ/mol, and −3.3 to −10.5 kJ/mol for B3LYP, M06-2X, and MP2. The models including Leu100 showed significant differences in the interaction energies for the B3LYP method as compared with the M06-2X and MP2 methods. The results revealed that the main

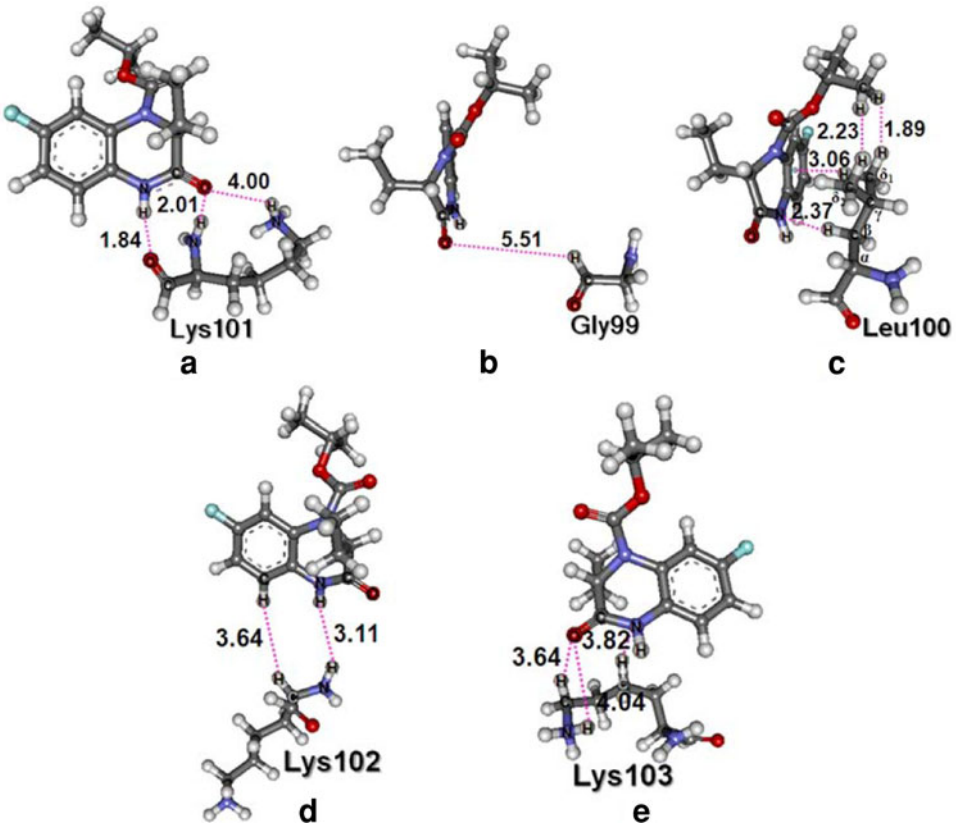

Fig. 3 Models of each residue (**a** Lys101, **b** Gly99, **c** Leu100, **d** Lys102, and **e** Lys103) interacting with GW420867X. Selected distances (Å) are shown

contribution of the attractive interaction to GW420867X is caused by the interaction with Lys101.

Effects of the side-chain of Lys101

The side-chain of Lys101 was modified to investigate which subunits contribute most to the attractive interactions to GW420867X. The interaction energies of these models are shown in Table 3. The comparison with model1-A0, in which the ammonium group is replaced by a methyl group, indicates that the charged ammonium moiety contributes to the main attractive interaction, increasing the interaction energies to 33.1, 32.6, and 32.2 kJ/mol at the B3LYP/6-31G(d), M06-2X/6-31G(d), and MP2/6-31G(d) levels. When the aliphatic side-chain was shortened, this did not cause a significant difference (<4 kJ/mol). Therefore, the results showed that the attractive interaction between GW420867X and Lys101 is mainly caused by the backbone and ammonium group of Lys101.

The effects of terminal NH and CO groups of Lys101

The peptide bond which has a partial double-bond character disappears when the model uses only a hydrogen atom to terminate at both sides of the residue's backbone. Because of the missing peptide bond character, the terminal NH and CO groups of Lys101 were varied to study the effect of terminal atoms when calculating the interaction energies. Model-R1A-D and model-R2A-D allow the evaluation of the terminating group effects at each terminal, as shown in Figs. 4 and 5. Model1-R1A-2A to model1-R1D-2D represent structures in which terminal groups were added at both terminals. Their interaction energies are presented in Table 4.

In the case of the terminal group attached to the carbonyl side, the distances between the added group and GW420867X revealed that the added groups on the carbonyl side have no pronounced effect. Compared with the interaction energy of model1-Lys101, the interaction energies of the other models (model1-R1A to model1-R1D) differ by about 1.7 to 7.5 kJ/mol, 1.7 to 8.4 kJ/mol, and 1.7 to 8.8 kJ/mol with B3LYP, M06-2X, and MP2. After expanding the size of the terminal group at the carbonyl end, the differences of the interaction energies are increased, but they tended to approach the interaction energy of model1-Lys101. As shown in model1-R1D, the differences of the interaction energies compared with model1-Lys101 are about −3.8, −4.6, and −5.9 kJ/mol with B3LYP, M06-2X, and MP2.

The effects are slightly larger for the termination of the amino side. Models representing the terminal group effects on the amino side (model1-R2A to model1-R2D) showed that the interaction energies differ from model1-Lys101 by about 1.7 to −10.5 kJ/mol, 1.3 to −10.5 kJ/mol, and 0.4 to

Table 3 Interaction energies between GW420867X and modified side-chain group of Lys101

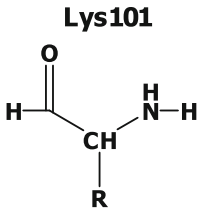

Model	R	Interaction energy (kJ/mol)		
		B3LYP/6-31G(d)	M06-2X/6-31G(d)	MP2/6-31G(d)
Model1-Lys101	$-(CH_2)_4-NH_3^+$	−65.3	−78.2	−68.2
Model1-A0	$-(CH_2)_4-CH_3$	−32.2	−45.6	−36.0
Model1-A1	$-(CH_2)_3-CH_3$	−32.2	−45.2	−35.6
Model1-A2	$-(CH_2)_2-CH_3$	−32.2	−45.2	−35.1
Model1-A3	$-CH_2-CH_3$	−31.8	−44.8	−34.3
Model1-A4	$-CH_3$	−31.0	−44.4	−33.5
Model1-A5	–H	−31.0	−42.7	−31.8

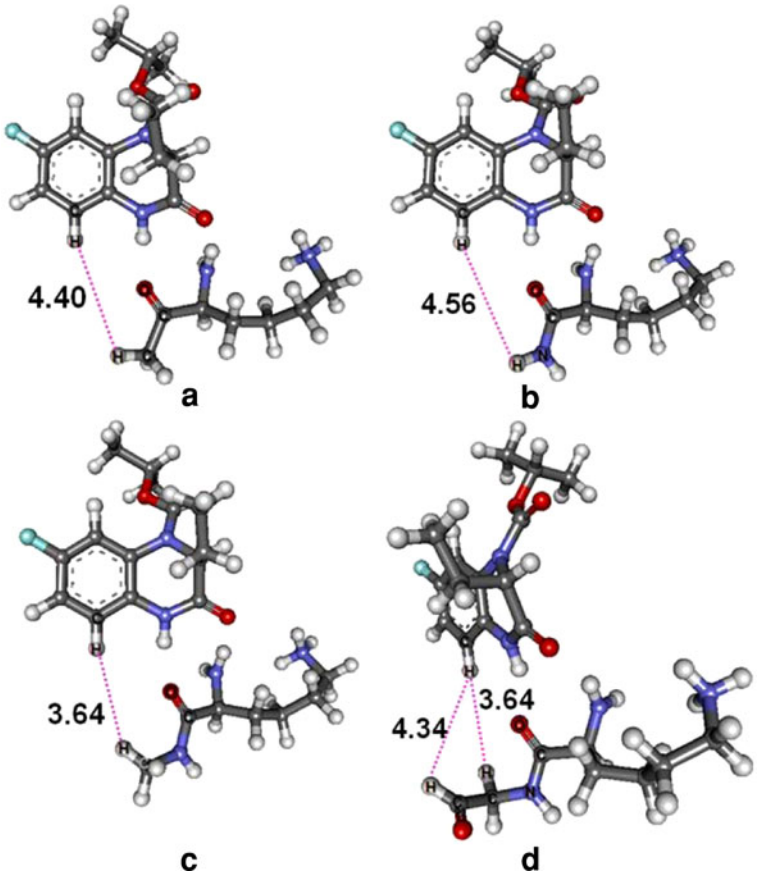

Fig. 4 Models representing the terminal group effects on the carbonyl group: **a** model1-R1A, **b** model1-R1B, **c** model1-R1C, and **d** model1-R1D. The distances (Å) between the added group and GW420867X are shown

−11.3 kJ/mol with B3LYP, M06-2X, and MP2. The interaction energies also revealed the same trend as shown in the case of the terminal carbonyl effect. The higher energy differences of the models representing the terminal group affects the amino side more than those on the carbonyl side, which may arise from the interaction caused by the added group. In the cases of the models with terminals on both sides (model1-R1A-2A to model1-R1D-2D), the results agree well with the models where a single terminal group is added on both sides.

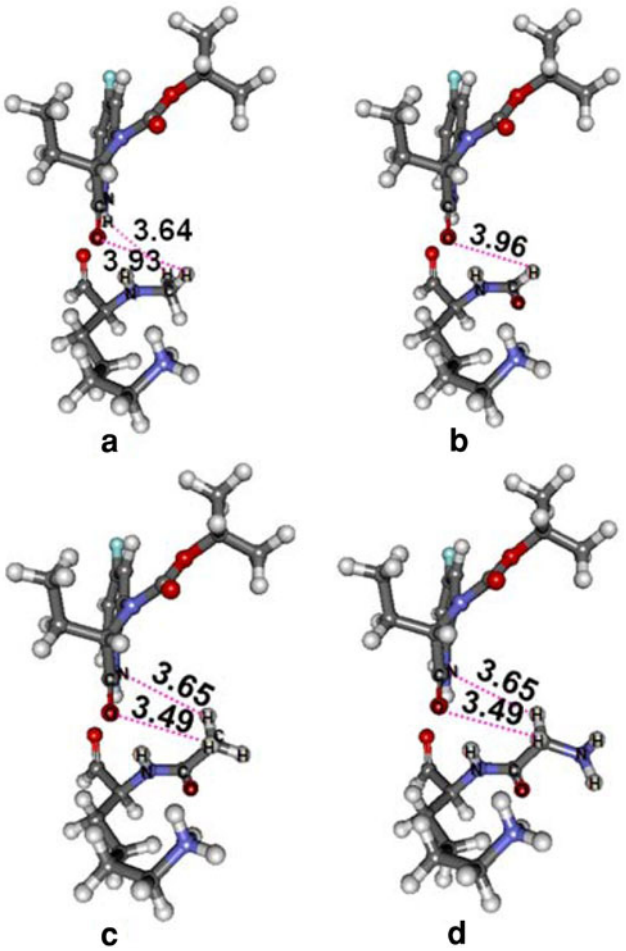

Fig. 5 Models representing the terminal group effects on the amino group: **a** model1-R2A, **b** model1-R2B, **c** model1-R2C, and **d** model1-R2D. The distances (Å) between the added group and GW420867X are shown

To explain the influence of the electrostatic contribution to the interaction energies, NPA charges on the oxygen atom of the carbonyl group and a hydrogen atom of the amino group in the backbone Lys101 are shown in Fig. 6. The results showed that NPA charges on the oxygen atom of Lys101 calculated by B3LYP and M06-2X are similar. The differences are about 0.01e. MP2 charges on the oxygen atom of Lys101 are about 0.1e more negative than those calculated by B3LYP and M06-2X. Charges on the oxygen atom of Lys101 in model1-Lys101 are also compared with those in the models including the peptide bond of both terminals of Lys101 (models3-1 and 5-1). The charges on the oxygen atom of Lys101 in models3-1 and 5-1 are more negative than those in model1-Lys101 by about 0.12e, 0.14e, and 0.15e for the B3LYP, M06-2X, and MP2 methods. However, charges on the oxygen atom of Lys101 in model3-1 are similar to those in model5-1. This may suggest that the peptide bond has an electrostatic effect on the models. In the case of the terminal group on the carbonyl side, model1-R1A, where a methyl group is added, no significant change of the charges to model1-Lys101 is observed. NPA charges on the oxygen atom of Lys101 in modelsR1B-D are close to those in models3-1 and 5-1 (<0.03e). In the cases of the models representing the terminal groups on the amino side (models1-R2A-D), the charge on the oxygen atom of Lys101 is not affected.

For atomic charges on the nitrogen atom of the amino group of Lys101, NPA charges on a nitrogen atom of amino group Lys101 showed similar values for all methods (<0.01e). The NPA charges in models3-1 and 5-1 are close to those in model-1 Lys101 (<0.03e). The terminal groups on the carbonyl and the amino sides have no influence on the charge at the nitrogen atom of the Lys101 amino group.

Effects of the side-chain of Leu100 and Lys102

To clarify the effect of the nearby residues, models with various residues at each terminal side were created. The interaction energies of the models are shown in Table 5. For the effects of side-chain Leu100, the B3LYP interaction energies showed that there was a repulsive interaction from both δ-carbon atoms of Leu100. The M06-2X and MP2 interaction energies showed no significant effects of the side-chain Leu100. In the case of the side-chain Lys102, no significant interaction energies were found for all three methods. The MP2 results showed that both side-chains of Leu100 and Lys102 did not affect the binding of GW420867X in the HIV-1 RT binding pocket.

Comparison between wild-type and Lys101Glu HIV-1 RT

The structures of the complexes of GW420867X with the wild-type and Lys101Glu mutant HIV-1 RT were compared by superimposing the backbone atoms. Their superimposed binding pockets are shown in Fig. 7. The orientation of GW420867X in the wild-type and Lys101Glu HIV-1 RT binding pockets is similar; however, the orientation of GW420867X in the Lys101Glu binding pocket shows a slight movement at ethyl and isopropoxy groups. Compared with Lys101, the side-chain of Glu101 is moved away from the binding pocket in order to avoid the repulsive interaction between carboxylic groups of Glu101 and Glu138(B). The backbone of Glu101 shows a slight deviation from that of Lys101. The conformation of Trp299 in the Lys101Glu binding pocket is found to be different from the conformation in the wild-type binding pocket. The movement of the phenyl ring plane of Tyr181 is also observed in the Lys101Glu binding pocket. The other residues in the Lys101 binding pocket reveal a slight shift from those in the wild-type binding pocket. The M06-2X and MP2 interaction energies between GW420867X and the

Table 4 Interaction energies between GW420867X and modified terminal groups of Lys101

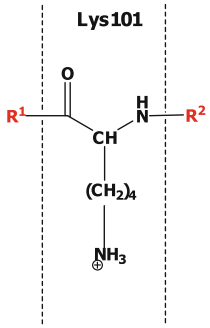

Model	R^1	R^2	Interaction energy (kJ/mol)		
			B3LYP/6-31G(d)	M06-2X/6-31G(d)	MP2/6-31G(d)
Model1-Lys101	H	H	−65.3	−78.2	−68.2
Terminal at carbonyl group					
Model1-R1A	$–CH_3$	H	−66.9 (−1.7)[a]	−79.9 (−1.7)	−69.9 (−1.7)
Model1-R1B	$–NH_2$	H	−72.8 (−7.5)	−86.6 (−8.4)	−76.6 (−8.4)
Model1-R1C	$–NH–CH_3$	H	−72.8 (−7.5)	−86.6 (−8.4)	−77.0 (−8.8)
Model1-R1D	$–NH–CH_2–CHO$	H	−69.0 (−3.8)	−82.8 (−4.6)	−74.1 (−5.9)
Terminal at amino group					
Model1-R2A	H	$–CH_3$	−63.6 (1.7)	−77.0 (1.3)	−67.8 (0.4)
Model1-R2B	H	–CHO	−75.7 (−10.5)	−88.7 (−10.5)	−79.5 (−11.3)
Model1-R2C	H	$–CO–CH_3$	−72.8 (−7.5)	−87.4 (−9.2)	−78.7 (−10.5)
Model1-R2D	H	$–CO–CH_2–NH_2$	−71.1 (−5.9)	−85.8 (−7.5)	−77.4 (−9.2)
Terminal at carbonyl and amino groups					
Model1-R1A-2A	$–CH_3$	$–CH_3$	−65.3 (0.0)	−78.2 (0.0)	−69.5 (−1.3)
Model1-R1A-2B	$–CH_3$	–CHO	−76.6 (−11.3)	−89.5 (−11.3)	−80.8 (−12.6)
Model1-R1A-2C	$–CH_3$	$–CO–CH_3$	−75.3 (−10.0)	−90.4 (−12.1)	−81.6 (−13.4)
Model1-R1A-2D	$–CH_3$	$–CO–CH_2–NH_2$	−72.4 (−7.1)	−87.4 (−9.2)	−79.5 (−11.3)
Model1-R1B-2A	$–NH_2$	$–CH_3$	−72.0 (−6.7)	−85.8 (−7.5)	−77.0 (−8.8)
Model1-R1B-2B	$–NH_2$	–CHO	−82.8 (−18.0)	−97.1 (−18.8)	−87.9 (−19.7)
Model1-R1B-2C	$–NH_2$	$–CO–CH_3$	−80.8 (−15.5)	−96.2 (−18.0)	−87.9 (−19.7)
Model1-R1B-2D	$–NH_2$	$–CO–CH_2–NH_2$	−79.1 (−13.8)	−94.6 (−16.3)	−86.6 (−18.4)
Model1-R1C-2A	$–NH–CH_3$	$–CH_3$	−71.5 (−6.3)	−85.8 (−7.5)	−77.0 (−8.8)
Model1-R1C-2B	$–NH–CH_3$	–CHO	−82.4 (−17.2)	−96.7 (−18.4)	−87.9 (−19.7)
Model1-R1C-2C	$–NH–CH_3$	$–CO–CH_3$	−80.3 (−15.1)	−95.8 (−17.6)	−87.9 (−19.7)
Model1-R1C-2D	$–NH–CH_3$	$–CO–CH_2–NH_2$	−78.7 (−13.4)	−94.6 (16.3)	−86.6 (−18.4)
Model1-R1D-2A	$–NH–CH_2–CHO$	$–CH_3$	−67.4 (−2.1)	−81.6 (−3.3)	−73.6 (−5.4)
Model1-R1D-2B	$–NH–CH_2–CHO$	–CHO	−78.7 (−13.4)	−92.5 (−14.2)	−84.5 (−16.3)
Model1-R1D-2C	$–NH–CH_2–CHO$	$–CO–CH_3$	−76.1 (−10.9)	−91.6 (−13.4)	−84.5 (−16.3)
Model1-R1D-2D	$–NH–CH_2–CHO$	$–CO–CH_2–NH_2$	−74.5 (−9.2)	−90.4 (−12.1)	−83.3 (−15.1)

[a] Energy difference, as compared with model1-Lys101

Lys101Glu binding pocket are presented in Table 6. The main difference between the interaction energies of the wild-type and Lys101Glu HIV-1 RT are found for residues Lys101 and Tyr181. GW420867X loses attractive interaction energies of 51.5 kJ/mol and 52.3 kJ/mol at M06-2X and MP2 because of mutation at residue 101. However, GW420867X still forms an attractive interaction with the backbone of Glu101. In the case of Tyr181 in the Lys101-Glu binding pocket, the movement of the side-chain Tyr181 may cause a repulsive interaction with the isopropoxy group of GW420867X, as shown by the increase of the interaction energies by about 60.7 and 66.5 kJ/mol at M06-2X and

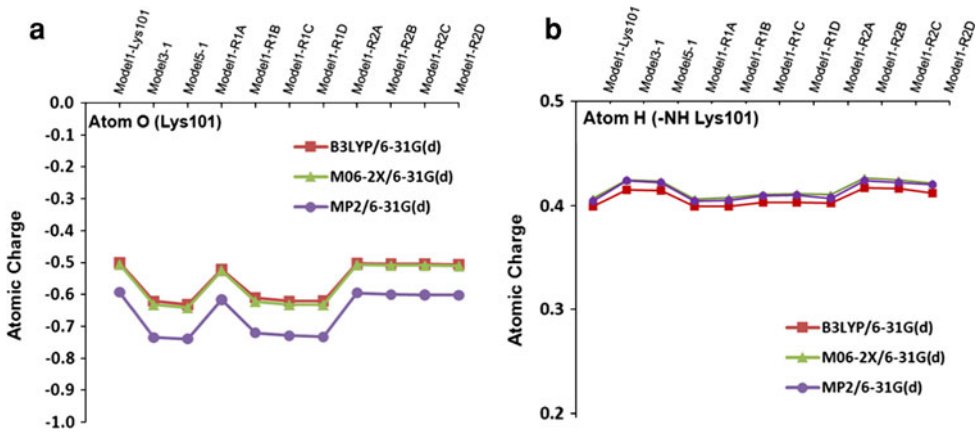

Fig. 6 Atomic charges on an oxygen atom (**a**) and a hydrogen atom (**b**) of backbone Lys101 of the models using only the residues

MP2, respectively. For the other residues, the results show no significant stabilization energies. From Table 6, the decrease of the attractive interaction with Glu101 and the increase of repulsive interaction with Tyr181 of GW420867X can explain why GW420867X loses binding affinity in the Lys101Glu HIV-1 RT complex.

To study the efficiency of interaction energy calculations performed by choosing individual amino acids, the

Table 5 Interaction energies between GW420867X and Lys101 and modified side-chains of Leu100 and Lys102

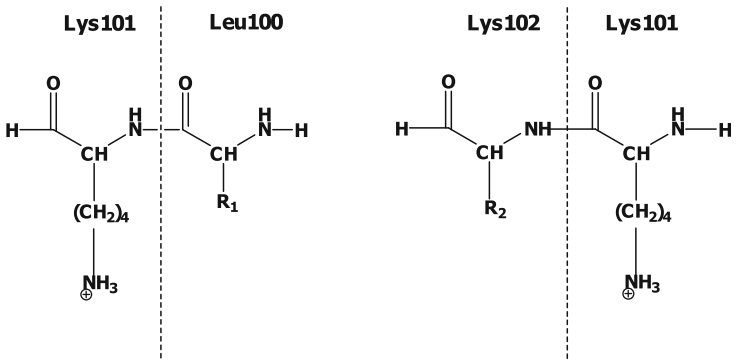

Model		Interaction energy (kJ/mol)		
		B3LYP/6-31G(d)	M06-2X/6-31G(d)	MP2/6-31G(d)
Model1-Lys101		−65.3	−78.2	−68.2
Model1-Leu100		24.7	−10.0	0.8
Model1-Lys102		6.3	5.9	4.6
	R_1			
Model2-1-Lys101Leu100	$-CH_2CH(CH_3)_2$	−43.5	−89.5	−70.7
Model2-1-A1	$-(CH_2)_2-CH_3(\delta_1)$	−55.2	−89.5	−77.0
Model2-1-A2	$-(CH_2)_2-CH_3(\delta_2)$	−52.3	−85.8	−72.0
Model2-1-A3	$-CH_2-CH_3$	−63.2	−87.0	−77.8
Model2-1-A4	$-CH_3$	−64.0	−84.5	−74.5
Model1-R2D	H	−43.5	−89.5	−70.7
	R_2			
Model2-2-Lys101Lys102	$-(CH_2)_4-NH_3^+$	−65.3	−78.7	−69.9
Model2-2-A1	$-(CH_2)_3-CH_3$	−69.5	−83.3	−74.5
Model2-2-A2	$-(CH_2)_2-CH_3$	−69.5	−83.3	−74.5
Model2-2-A3	$-CH_2-CH_3$	−69.5	−82.8	−74.5
Model2-2-A4	$-CH_3$	−69.5	−82.8	−74.5
Model1-R1D	H	−69.0	−82.8	−74.1

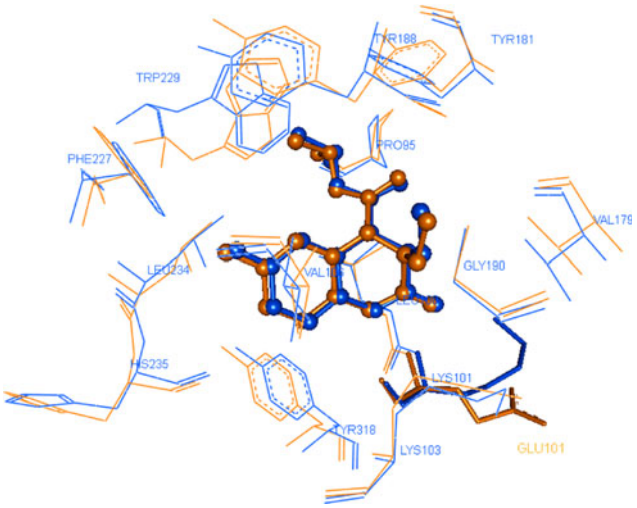

Fig. 7 Superimposition of GW420867X (ball-and-stick model) binding pocket between wild-type (*blue*) and Lys101Glu (*orange*) HIV-1 RT [Lys101 (*blue*) and Glu101 (*orange*) are shown in stick models] (color figure online)

interaction energy of GW420867X in the WT and Lys101Glu HIV-1 RT binding pocket was also calculated. Their interaction energies are −177.8 and −50.6 kJ/mol for WT and Lys101Glu HIV-1 RT. The interaction energies confirm that GW420867X binds better to WT HIV-1 RT than to Lys101Glu HIV-1 RT. The deviation of the interaction energy between WT and Lys101Glu HIV-1 RT is 127.2 kJ/mol. In addition, as compared with the interaction energy of GW420867X in the binding pocket, the deviation of the summation of the individual interaction energies by M06-2X/6-31G(d) and MP2/6-31G(d) methods are close to that of the interaction energy in the binding pocket. The difference of the interaction energies are about 11.7 and 4.2 kJ/mol by M06-2X/6-31G(d) and MP2/6-31G(d) methods, respectively. Consequently the interaction energy between GW420867X and individual amino acids in the binding pocket can be used to explain the binding affinity of GW420867X.

Methods

The structures of wild-type and Lys101Glu HIV-1 RT co-crystallized with GW420867X were obtained from the protein data bank (pdb codes 2opp and 2opr) [8]. The structures of wild-type and Lys101Glu HIV-1 RT and GW420867X were extracted, and then the hydrogen atoms were added using the SYBYL 7.2 program [25]. Amino acids which have any atoms close to GW420867X within 4 Å were selected to study their interaction profile to GW420867X. The 14 selected amino acids were Pro95,

Table 6 Interaction energies by M06-2X/6-31G(d) and MP2/6-31G(d) methods between GW420867X and surrounding residues in wild-type and Lys101Glu HIV-1 RT

Model	Interaction energy (kJ/mol)					
	M06-2X/6-31G(d)			MP2/6-31G(d)		
	Wild-type	Lys101Glu	ΔE^a	Wild-type	Lys101Glu	ΔE^a
Pro95	4.2	−2.9	−7.1	8.4	−2.5	−10.9
Leu100	−10.0	−10.9	−0.8	0.8	0.4	−0.4
Lys101/Glu101	−78.2	−26.8	51.5	−68.2	−15.9	52.3
Lys103	−25.1	−31.8	−6.7	−26.8	−30.1	−3.3
Val106	−5.0	−3.3	1.7	−3.8	−0.8	2.9
Val179	−9.2	1.7	10.9	−3.8	6.7	10.5
Tyr181	−10.5	50.2	60.7	−10.0	56.5	66.5
Tyr188	−7.5	−2.9	4.6	−7.9	1.3	9.2
Gly190	−3.8	1.7	5.4	−1.3	7.9	9.2
Phe227	−1.3	−2.9	−1.7	−2.5	−4.6	−2.1
Trp229	−10.5	−10.5	0.0	−7.1	−9.2	−2.1
Leu234	−4.2	−3.8	0.4	−5.4	−4.2	1.3
His235	−7.5	−8.4	−0.8	−6.7	−8.4	−1.7
Tyr318	−7.9	−10.5	−2.5	−10.0	−10.0	0.0
Total	−176.6	−61.1	115.5	−144.3	−13.0	131.4
Binding pocket (14 amino acids)	−177.8	−50.6	127.2	–	–	–

[a] $\Delta E = \text{I.E.}_{\cdot\text{Lys101Glu}} - \text{I.E.}_{\cdot\text{wild-type}}$

Leu100, Lys/Glu101, Lys103, Val106, Val179, Tyr181, Tyr188, Gly190, Phe227, Trp229, Leu234, His235, and Tyr318. To study the individual interaction energies of each amino acid, the amino acids were terminated with hydrogen atoms at the C- and N-terminals. These interaction energies were calculated using B3LYP, M06-2X, and MP2 methods with 6-31G(d), 6-31G(d,p), 6-311G(d), and 6-311G(d,p) basis sets. All calculations were performed with Gaussian03 [26]. Correction for basis set superposition error (BSSE) was applied. The interaction energy (INT) between GW420867X and each amino acid was defined as follows: INT = E(GW420867X + residue) − [E(GW420867X) + E(residue)]. E(GW420867X + residue) is the energy of the complex between GW420867X and the amino acid residue. E(GW420867X) and E(residue) are the energies of GW420867X and the residues. In detail, the influence of neighboring residues of Lys101 was investigated by including one or two residues at both the C- and N-terminal of Lys101 into the models. Models varying the size of the Lys101 side-chain were constructed to investigate the specificity of the attractive interaction. The size of Leu100 and Lys102 side-chains were also varied to study their influence. These models were terminated with hydrogen atoms. In the case of the effects of terminal atoms, some functional groups using the position of nearby residues were added to the C- and N-terminals of Lys101. In addition, a population analysis method, natural population analysis (NPA), was used to study the electrostatic effect by calculating the NPA charges on a hydrogen atom (at an amino group) and an oxygen atom of backbone Lys101 using only the residues. Furthermore, the interaction energy of GW420867X in the binding pocket including 14 amino acids of WT and K101E HIV-1 RT was calculated by M06-2X/6-31G(d,p) for comparison with the interaction energy obtaining by individual amino acids.

Acknowledgments The authors are grateful to the Thailand Research Fund (RTA53800010, DBG5180022, MRG5080267) and Faculty of Science (ScRF), Kasetsart University for the research grant. Center of Nanotechnology at Kasetsart University, Laboratory for Computational and Applied Chemistry (LCAC), National Center of Excellence for Petroleum, Petrochemicals, and Advanced Materials (NCE-PPAM), and Large Scale Simulation Research Laboratory (LSR)/NECTEC, ASEA-Uninet and the University of Vienna are also gratefully acknowledged for research facilities and computing resources.

References

1. Jacobo-Molina A, Arnold E (1991) Biochemistry 30:6351
2. Jacobo-Molina A, Ding J, Nanni RG, Clark AD Jr, Lu X, Tantillo C, Williams RL, Kamer G, Ferris AL, Clark P, Hizi A, Hughesi SH, Arnold E (1993) Proc Natl Acad Sci USA 90:6320
3. Balzarini J (1999) Biochem Pharmacol 58:1
4. Ren J, Stammers DK (2005) Trends Pharmacol Sci 26:4
5. De Clercq E (1998) Antiviral Res 38:153
6. Menéndez-Arias L (2002) Trends Pharmacol Sci 23:381
7. De Clercq E (2009) Int J Antimicrob Agents 33:307
8. Ren J, Nichols CE, Chamberlain PP, Weaver KL, Short SA, Chan JH, Kleim JP, Stammers DK (2007) J Med Chem 50:2301
9. Nunrium P, Kuno M, Saen-oon S, Hannongbua S (2005) Chem Phys Lett 405:198
10. Saen-oon S, Kuno M, Hannongbua S (2005) Proteins 61:859
11. Mei Y, He X, Xiang Y, Zhang DW, Zhang JZH (2005) Proteins 59:489
12. He X, Mei Y, Xiang Y, Zhang DW, Zhang JZH (2005) Proteins 61:423
13. Zhao Y, Truhlar DG (2008) Theor Chem Account 120:215
14. Zhao Y, Truhlar DG (2008) Account Chem Res 41:157
15. Gu J, Wang J, Leszczynski J, Xie Y, Schaefer HF III (2008) Chem Phys Lett 459:164
16. Mourik TV (2008) J Chem Theory Comput 4:1610
17. Sitkoff D, Lockhart DJ, Sharp KA, Honig B (1994) Biophys J 67:2251
18. Baeten A, Maes D, Geerlings P (1998) J Theor Biol 195:27
19. Roos G, Messens J, Loverix S, Wyns L, Geerlings P (2004) J Phys Chem B 108:17216
20. Kang YK, Scheraga HA (2008) J Phys Chem B 112:5470
21. Martin F, Zipse H (2005) J Comput Chem 26:97
22. Tsuzuki S, Lüthi HP (2001) J Chem Phys 114:3949
23. Kuno M, Hannongbua S, Morokuma K (2003) Chem Phys Lett 380:456
24. Saparpakorn P, Hannongbua S, Rognan D (2006) SAR QSAR Environ Res 17:183
25. SYBYL 7.2, TRIPOS, Assoc., Inc., St. Louis, MO
26. Frisch MJ, Trucks GW, Schlegel HB, Scuseria GE, Robb MA, Cheeseman JR, Montgomery JA Jr, Vreven T, Kudin KN, Burant JC, Millam JM, Iyengar SS, Tomasi J, Barone V, Mennucci B, Cossi M, Scalmani G, Rega N, Petersson GA, Nakatsuji H, Hada M, Ehara M, Toyota K, Fukuda R, Hasegawa J, Ishida M, Nakajima T, Honda Y, Kitao O, Nakai H, Klene M, Li X, Knox JE, Hratchian HP, Cross JB, Bakken V, Adamo C, Jaramillo J, Gomperts R, Stratmann RE, Yazyev O, Austin AJ, Cammi R, Pomelli C, Ochterski JW, Ayala PY, Morokuma K, Voth GA, Salvador P, Dannenberg JJ, Zakrzewski VG, Dapprich S, Daniels AD, Strain MC, Farkas O, Malick DK, Rabuck AD, Raghavachari K, Foresman JB, Ortiz JV, Cui Q, Baboul AG, Clifford S, Cioslowski J, Stefanov BB, Liu G, Liashenko A, Piskorz P, Komaromi I, Martin RL, Fox DJ, Keith T, Al-Laham MA, Peng CY, Nanayakkara A, Challacombe M, Gill PMW, Johnson B, Chen W, Wong MW, Gonzalez C, Pople JA (2004) Gaussian 03. Gaussian, Inc., Wallingford